International Journal of Pharmaceutics 425 (2012) 35–43

Contents lists available at SciVerse ScienceDirect

International Journal of Pharmaceutics

journal homepage: www.elsevier.com/locate/ijpharm

Pharmaceutical Nanotechnology

Dextran–protamine–solid lipid nanoparticles as a non-viral vector for gene therapy: *In vitro* characterization and *in vivo* transfection after intravenous administration to mice

Diego Delgado[a], Alicia Rodríguez Gascón[a], Ana del Pozo-Rodríguez[a], Enrique Echevarría[b], Aritz Pérez Ruiz de Garibay[a], Juan Manuel Rodríguez[b], Maria Ángeles Solinís[a,*]

[a] *Pharmacy and Pharmaceutical Technology Laboratory, Pharmacy Faculty, University of the Basque Country (UPV-EHU), Paseo de la Universidad 7, 01006 Vitoria-Gasteiz, Spain*
[b] *Physiology Laboratory, Pharmacy Faculty, University of the Basque Country (UPV-EHU), Paseo de la Universidad 7, 01006 Vitoria-Gasteiz, Spain*

ARTICLE INFO

Article history:
Received 30 October 2011
Received in revised form
23 December 2011
Accepted 25 December 2011
Available online 31 December 2011

Keywords:
Solid lipid nanoparticles
Gene therapy
Endocytosis
Intracellular trafficking
In vivo transfection
Non-viral vectors

ABSTRACT

The aim of present work is to evaluate the transfection capacity of a new multicomponent system based on dextran (Dex), protamine (Prot), and solid lipid nanoparticles (SLN) after intravenous administration to mice. The vectors containing the pCMS-EGFP plasmid were characterized in terms of particle size and surface charge. *In vitro* transfection capacity and cell viability were studied in four cell lines, and compared with the transfection capacity of SLN without dextran and protamine. Transfection capacity was related to the endocytosis mechanism: caveolae or clathrin. The Dex–Prot–DNA–SLN vector showed a higher transfection capacity in those cells with a high ratio of activity of clathrin/caveolae-mediated endocytosis. However, the complex prepared without dextran and protamine (DNA–SLN) was more effective in those cells with a high ratio of activity of caveolae/clathrin-mediated endocytosis. The interaction with erythrocytes and the potential hemolytic effect were also checked. The Dex–Prot–DNA–SLN vector showed no agglutination of erythrocytes, probably due to the presence of dextran. After intravenous administration to BALB/c mice, the vector was able to induce the expression of the green fluorescent protein in liver, spleen and lungs, and the protein expression was maintained for at least 7 days. Although additional studies are necessary, this work reveals the promising potential of this new gene delivery system for the treatment of genetic and non-genetic diseases through gene therapy.

1. Introduction

Non-viral delivery systems possess features that result advantageous for their use in gene therapy: safety, low-cost production, high-reproducibility and no limit size of DNA to transport (del Pozo-Rodríguez et al., 2011). However, the use of non-viral vectors is limited by their low transfection efficacy, and the search for methods to optimize them is essential to reach the efficacy of gene therapy mediated viral vectors.

Efforts to improve non-viral constructs have been made following different strategies, and the combination of several constituents to form hybrid systems has been the most extended and successful approach. The interaction between cationic lipids and DNA, by means of their opposite charges, to form complexes (lipoplexes) (Ma et al., 2007) stands out as one of the most promising systems. This technique has been employed in several clinical trials to treat diseases such as cystic fibrosis (Porteous et al., 1997; Noone et al., 2000) and cancer (Yoshida et al., 2004) and, thus, cationic lipids seem to be the key compound to develop multicomponent carriers (Koyanova and Tenchov, 2011). In order to enhance the transfection efficacy of these lipids, they can be associated with cell penetrating peptides (CPPs), such as the transcriptional activator protein (TAT) (Gupta et al., 2007) or the Sweet Arrow Peptide (SAP) (del Pozo-Rodríguez et al., 2009), which have been used for gene delivery (Gupta et al., 2005). Different mechanisms are used for cellular uptake: endocytosis *via* clathrin, endocytosis *via* caveolae/lipids-raft, clathrin/caveolae-independent endocytosis, *etc.* The use of constituents that modulate these pathways leads to an improvement in transfection of the gene delivery systems (Rejman et al., 2005; Delgado et al., 2012). Another strategy consists in facilitating the endosomal escape before the degradation of the vector by using polymers such as polyethylenimine or chemicals such as chloroquine, which rupture the endosome when the pH is modified (Varkouhi et al., 2010). The nuclear membrane is the last barrier in the transfection process and it can be overcome by means of peptides with nuclear localization signals (NLS). These peptides have the ability to translocate the DNA

* Corresponding author. Tel.: +34 945 01 34 69.
E-mail address: marian.solinis@ehu.es (M.Á. Solinís).

0378-5173/$ – see front matter © 2011 Elsevier B.V. All rights reserved.
doi:10.1016/j.ijpharm.2011.12.052

through the nuclear membrane (Zanta et al., 1999) and they have shown a good response when associated to lipid-based systems (Hoare et al., 2010).

Besides intracellular obstacles, there are specific problems associated with intravenous administration naked DNA. Both digestion by nucleases and hepatic uptake clearance can entail a quick DNA elimination from circulation. Although this drawback may be overcome by using gene delivery systems (Liu et al., 2007), these present another handicap related to positive charge, which causes aggregation and hemagglutination processes that may condition transfection and toxicity (Finsinger et al., 2000; Eliyahu et al., 2002). Including polymers with "shielding" properties over positive charges, such as poly(ethylene glycol) (PEG), overcomes the interaction with some components of blood such as erythrocytes, leading to an extended stay of the vector in the organism (Morille et al., 2008).

As a follow-up to previous studies, we have designed new complexes based on solid lipid nanoparticles (SLN), protamine (Prot), a NLS peptide, and dextran (Dex), an anionic polysaccharide (Gascón et al., 2011). This new vector was previously assayed in rats after ocular administration and it showed a significant transfection of different ocular tissues (Delgado et al., 2012). The objective of the present work was to evaluate this new gene delivery system *in vitro* in four cell lines and *in vivo* after intravenous administration to mice.

2. Materials and methods

2.1. Materials

Precirol® ATO 5 (glyceryl palmitostearate) was provided by Gattefossé (Madrid, Spain). Nile Red, protamine sulphate salt from salmon (Grade X), dextran (M_n = 3260), and Triton® X-100 were purchased from Sigma–Aldrich (Madrid, Spain). Tween 80 was provided by Vencaser (Bilbao, Spain) and dichloromethane by Panreac (Barcelona, Spain). 1,2-Dioleoyl-3-trimethylammonium-propane chloride salt (DOTAP) was obtained from Avanti Polar Lipids, Inc.

Plasmid pCMS-EGFP encoding the enhanced green fluorescent protein (EGFP) was purchased from BD Biosciences Clontech (Palo Alto, US) and amplified by Dro Biosystems S.L. (San Sebastián, Spain).

Cell culture reagents were purchased from LGC Promochem (Barcelona, Spain). Antibiotic Normocin™ was obtained from InvivoGen (San Diego, California, US). BD Viaprobe kit was provided by BD Biosciences (Belgium). AlexaFluor488-Cholera toxin and AlexaFluor488-Transferrin were provided by Molecular Probes (Barcelona, Spain), and Fluoromount G by SouthernBiotech (Coultek, España).

Female BALB/c nude mice weighing 18–22 g (5 weeks of age) were purchased from Harlam Interfauna Ibérica S.L. (Barcelona, Spain).

Primary antibody (polyclonal anti-GFP, IgG fraction) and secondary antibody (Alexa Fluor® 488 goat anti-rabbit IgG) were provided by Invitrogen (Barcelona, Spain), and the normal goat serum (NGS) from Chemicon International Inc. (Temecula, CA, USA).

2.2. Production of vectors

The SLN were produced by a solvent emulsification–evaporation technique, previously described by del Pozo-Rodríguez et al. (2007). Briefly, Precirol® ATO 5 was dissolved in dichloromethane (5%, w/v), and then emulsified in an aqueous phase containing DOTAP (0.4%, w/v) and Tween 80 (0.1%, w/v). The emulsion was obtained by sonication (Branson Sonifier 250, Danbury) for 30 s at 50 W, and after the evaporation of the organic solvent an SLN suspension was formed upon solidification of the Precirol® ATO 5 in the aqueous medium. Finally, the SLN were washed by centrifugation (3000 rpm, 20 min, 3×) using Millipore (Madrid, Spain) Amicon® Ultra centrifugal filters (100,000 MWCO).

DNA–SLN vectors were obtained by mixing the pCMS-EGFP plasmid with an aqueous suspension of SLN under agitation for 30 min, which allows the formation of electrostatic interactions between the positive charges of SLN and the negative charges of DNA. The SLN to DNA ratio, expressed as the ratio DOTAP to DNA (w/w), was fixed at 5:1, which has previously demonstrated to fully condense DNA (del Pozo-Rodríguez et al., 2007, 2008).

In order to elaborate the Dex–Prot–DNA–SLN vector, an aqueous solution of dextran was mixed with and aqueous solution of protamine to form the Dex–Prot complexes at w/w ratio of 1:2. Then, the pCMS-EGFP plasmid was bound to the Dex–Prot complexes to set Dex–Prot–DNA ratios of 1:2:1 (w/w/w). Finally, Dex–Prot–DNA complexes were mixed with SLN suspension under agitation for 30 min at w/w/w/w ratio of 1:2:1:5. Interaction between free negative charges of DNA and positive charges of SLN led to the formation of the vectors, in which Dex–Prot–DNA complexes are adsorbed on the nanoparticle surface.

2.3. Size and ζ potential measurements

The size of vectors was determined by photon correlation spectroscopy (PCS), given in volume distribution. ζ potential was measured by laser Doppler velocimetry (LDV). Both measurements were performed on a Malvern Zetasizer 3000 (Malvern Instruments, Worcestershire, UK). Samples were diluted in 0.1 mM NaCl (aq.).

2.4. In vitro transfection

In vitro assays were performed with human embryonic kidney (HEK-293) cell line, human umbilical vein (Ea.hy926) cell line, hepatocellular carcinoma (Hep G2) cell line and human retinal epithelium pigment (ARPE-19) cell line, obtained from the American Type Culture Collection (ATCC).

HEK-293 cells were maintained in Eagle's Minimal Essential Medium with Earle's BSS and 2 mM L-glutamine (EMEM) supplemented with 10% heat-inactivated horse serum and 1% Normocin™. Cells were incubated at 37 °C with 5% CO_2 in air and subcultured every 2–3 days using trypsin/EDTA. For transfection HEK-293 cells were seeded on 24 well plates at density of 150,000 per well and allowed to adhere overnight.

Ea.hy926 cells were maintained in Dulbecco's Modified Eagle's Medium (D-MEM) supplemented with 10% heat-inactivated fetal calf serum, HAT supplement 1× and 1% Normocin™. Cells were incubated at 37 °C with 5% CO_2 in air and subcultured every 2–3 days using trypsin/EDTA. For transfection Ea.hy926 cells were seeded on 24 well plates at density of 60,000 per well and allowed to adhere overnight.

Hep G2 cells were maintained in Eagle's Minimal Essential Medium (EMEM) supplemented with 10% heat-inactivated fetal calf serum and 1% Normocin™. Cells were incubated at 37 °C with 5% CO_2 in air and subcultured every 2–3 days using trypsin/EDTA. For transfection Hep G2 cells were seeded on 24 well plates at density of 120,000 per well and allowed to adhere overnight.

ARPE-19 cells were maintained in Dulbecco's Modified Eagle's Medium–Han's Nutrient Mixture F-12 (1:1) medium (D-MEM/F12) supplemented with 10% heat-inactivated fetal calf serum and 1% Normocin™. Cells were incubated at 37 °C with 5% CO_2 in air and subcultured every 2–3 days using trypsin/EDTA. For transfection ARPE-19 cells were seeded on 12 well plates at density of 30,000 per well and allowed to adhere overnight.

The formulations were diluted in HBS and added to the cell cultures. In all cases, 2.5 μg of DNA were added. The cells were incubated with the vectors at 37 °C, and after 4 h, the medium containing the complexes in the wells was refreshed with 1 mL of complete medium. The cells were then allowed to grow for another 72 h.

As control, the DNA–SLN vector without Dex–Prot whose transfection ability was evaluated in previous works (del Pozo-Rodríguez et al., 2007, 2008) was also assayed.

2.5. Flow cytometry mediated analysis of transfection efficacy and cell viability

At the end of the incubation period, the cells were washed once with 300 μL of PBS, and then detached with 400 μL of 0.05% trypsin–EDTA. The cells were then centrifuged at 1500 × *g*, and resuspended with PBS and directly introduced into a FACSCalibur flow cytometer (Becton Dickinson Biosciences, San Jose, CA, US). For each sample, 10,000 events were collected.

Transfection efficacy was quantified by measuring the fluorescence of EGFP at 525 nm (FL1). For cell viability measurements, the BD Via-Probe kit was employed. The reagent (5 μL) was added to each sample, and after 10 min of incubation, the fluorescence corresponding to dead cells was measured at 650 nm (FL3).

2.6. Cellular uptake

The entry of vectors into the cells was studied quantitatively by flow cytometry. For this purpose SLN were labeled with the fluorescent dye Nile Red (λ = 590 nm) according to a previously reported method (Borgia et al., 2005). Briefly, Nile Red was incorporated into the dichloromethane employed to prepare SLN by the emulsification–evaporation technique described above.

Two hours after the addition of vectors, cells were washed three times with PBS and detached from plates. Cells incorporating either DNA–SLN or Dex–Prot–DNA–SLN vectors labeled with Nile Red were quantified by flow cytometry at 650 nm (FL3). For each sample, 10,000 events were collected.

2.7. Endocytosis activity

The endocytic processes present in each cell line were analyzed by flow cytometry studies with AlexaFluor488-Cholera Toxin and AlexaFluor488-Transferrin, which are markers of caveolae-mediated endocytosis and clathrin-mediated endocytosis, respectively. Cells were seeded in the same conditions described in Section 2.4 and allowed to adhere overnight. Markers were added to the cell cultures and cells were then incubated with the markers at 37 °C. After 2 h, the endocytosis activity of each marker was quantified by flow cytometry measuring the fluorescence of AlexaFluor488 at 525 nm (FL1).

2.8. Interaction with erythrocytes

2.8.1. Hemagglutination assay

A hemolysis assay was conducted following the protocol previously described by Kurosaki et al. (2010). Briefly, fresh human blood of the 0^+ type was centrifuged at 4000 rpm for 5 min and the plasma and the buffy coat were discarded. Erythrocytes were washed three times by centrifugation at 4000 rpm and were diluted in PBS to a final concentration of 2% (v/v). Naked plasmid, DNA–SLN and Dex–Prot–DNA–SLN vectors were added to erythrocytes suspension at ratio 1:1 (v/v) and incubated for 15 min at room temperature. The sample was placed on a microscope slide and hemagglutination was observed by microscopy.

2.8.2. Hemolysis assay

A hemolysis assay was conducted following the protocol previously described by Kurosaki et al. (2010). Briefly, fresh human blood of the 0^+ type was centrifuged at 4000 rpm for 5 min and the plasma and the buffy coat were discarded. Erythrocytes were washed three times with PBS by centrifugation at 4000 rpm and were diluted in PBS to a final concentration of 5% (v/v). Naked plasmid, DNA–SLN and Dex–Prot–DNA–SLN vectors were added to erythrocytes suspension at ratio 1:1 (v/v) and incubated for 60 min at room temperature. Then, suspensions were centrifuged at 4000 rpm during 5 min and supernatants were taken to quantify the hemolysis by measuring haemoglobin release at 545 nm in a microplate reader. A lysis buffer was employed for the 100% hemolysis sample.

2.9. Intravenous administration

Animals were handled in accordance with the Principles of Laboratory Animal Care (http://www.history.nih.gov/laws). Mice were quarantined for approximately 1 week prior to the study. They were housed under standard conditions and had *ad libitum* access to water and standard laboratory rodent diet. Following the standard procedure, the Dex–Prot–DNA–SLN vectors were injected into the tail vein in a volume of 100 μL (60 μg of plasmid). Controls were employed by administering free DNA and SLN without plasmid in the same way and volume. The treatment was administered to three mice in each group. Three and 7 days post-injection mice were sacrificed and the liver, lungs and spleen were removed, quick frozen in liquid nitrogen embedded in tissue freezing medium (Jung, Leica) and thin sectioned on a cryostat (Cryocut 3,000, Leica).

2.9.1. Immunolabelling of EGFP in tissue sections

Cryostat sections (8 μm) were fixed with 4% paraformaldehyde during 10 min at room temperature. Following washing in PBS, sections were blocked and permeabilized in PBS 0.1 M, 0.1% Triton® X-100 and 2% normal goat serum (NGS) for 1 h at room temperature. Then, sections were incubated in primary antibody (polyclonal anti-GFP, IgG fraction) for 2 h at room temperature. Following adequate washing in PBS, sections were incubated in secondary antibody (Alexa Fluor® 488 goat anti-rabbit IgG). Finally, sections were washed again in PBS and coverslipped with Fluoromount G.

Images of the immunolabeled sections were captured with an inverted microscopy equipped with an attachment for fluorescent observation (model EclipseTE2000-S, Nikon). Results were expressed as the percentage of sections in which EGFP was detected.

2.10. Statistical analysis

Results are reported as mean values (S.D. = standard deviation). Statistical analyses were performed with SPSS 17.0 (SPSS®, Chicago, IL, USA). The normal distribution of samples was assessed by the Shapiro–Wilk test, and homogeneity of variance by the Levene test. The different formulations were compared with ANOVA and Student's *t* test. Differences were considered statistically significant at $p < 0.05$.

3. Results

3.1. Size and zeta potential measurements

The DNA–SLN vector and the Dex–Prot–DNA–SLN vector showed sizes around 284 nm, and zeta potential about +30 mV, respectively (Table 1). The presence of dextran and protamine in

Table 1
Size, zeta potential and polydispersion index of the DNA–SLN and the Dex–Prot–DNA–SLN vector.

	DNA–SLN	Dex–Prot–DNA–SLN
Size (nm)	283.63 ± 10.68	284.23 ± 11.87
Zeta potential (mV)	34.35 ± 6.62	30.60 ± 6.47
Polydispersion Index	0.42 ± 0.03	0.26 ± 0.02

the formulation did not result in statistically significant differences in size or zeta potential ($p > 0.05$).

3.2. In vitro transfection and cell viability

We first checked that the Dex–Prot–DNA complex (without SLN) was unable to transfect (data not show). Fig. 1A shows the percent of cells transfected 72 h after the addition of vectors assayed: DNA–SLN and Dex–Prot–DNA–SLN. In HEK-293 cells, the DNA–SLN vector induced a high transfection level (49.59 ± 2.07%); however, the same vector induced lower transfection in the other three cell lines (≤10%). Regarding the Dex–Prot–DNA–SLN vector, the highest transfection level was reached in ARPE-19 cells (48.03 ± 2.83%); in the other cell lines, transfection was significantly lower, especially in HEK-293 cells.

Cell viability, measured at 72 h was over 80% in all cell lines and it was significantly higher with the Dex–Prot–DNA–SLN vector in HEK-293, ARPE-19 and Ea.hy926 cells ($p < 0.05$) than with the DNA–SLN vector (Fig. 1B).

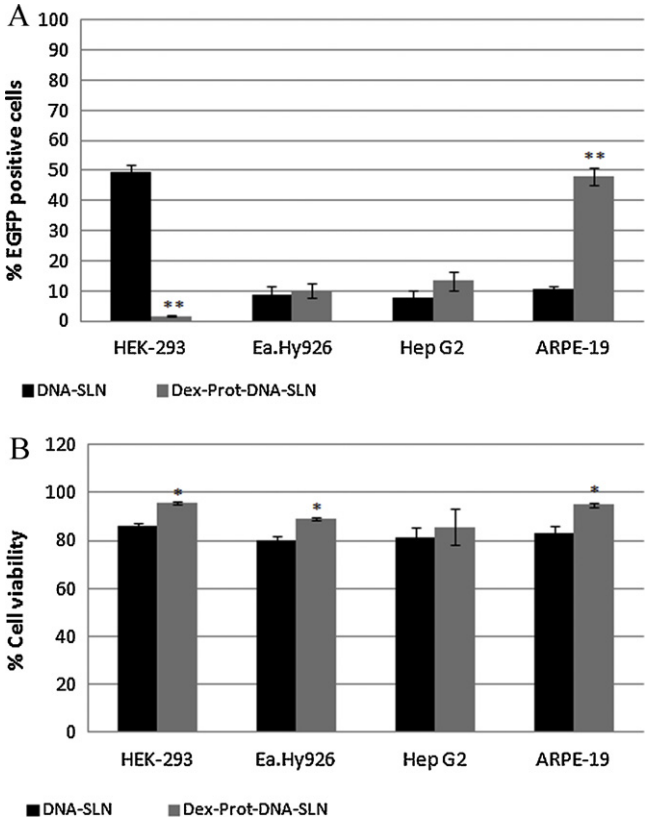

Fig. 1. Transfection (A) and cell viability (B) for each formulation assayed in the different cell lines 72 h after the addition of vectors. The SLN to DNA ratio (w/w) was 5:1 and the dextran–protamine to DNA ratio 1:2:1. Error bars represent S.D. ($n = 9$). $^{**}p < 0.01$ with respect to DNA–SLN formulation; $^{*}p < 0.05$ with respect to DNA–SLN formulation.

3.3. Cellular uptake

In all cell lines, both vectors showed a high entry into cells as Fig. 2 shows. The presence of the Dex–Prot complex in the nanoparticles led to a slight decrease in the cellular uptake in HEK-293 and Ea.hy926 cells. This is shown by a higher rightward shift of the histogram obtained from the cells treated with the DNA–SLN vector (Fig. 2A and B). No differences between the formulations were detected in the other cell lines.

3.4. Endocytosis activity

After treating the cells with the caveolae-mediated endocytosis marker, the highest activity was observed in HEK-293 cells (Fig. 3A). The marker uptake in Ea.hy926, Hep G2 and ARPE-19

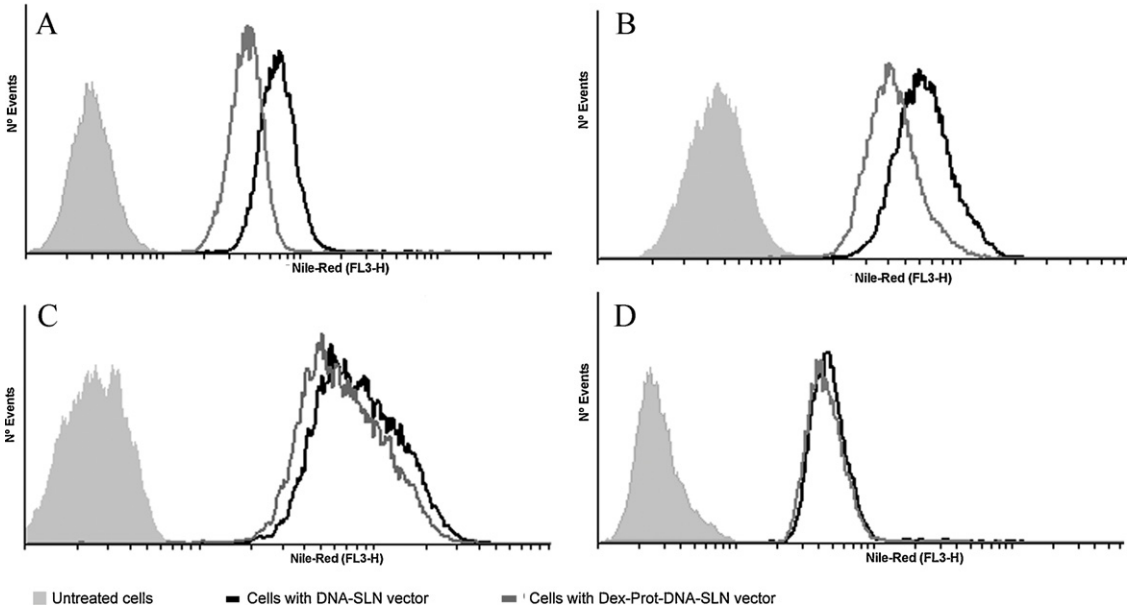

Fig. 2. Flow cytometry analysis of the cellular uptake study of the DNA–SLN vector and the Dex–Prot–DNA–SLN vector in HEK-293 cells (A), Ea.Hy926 cells (B), Hep G2 cells (C) and ARPE-19 cells (D). Vectors were labeled with Nile Red.

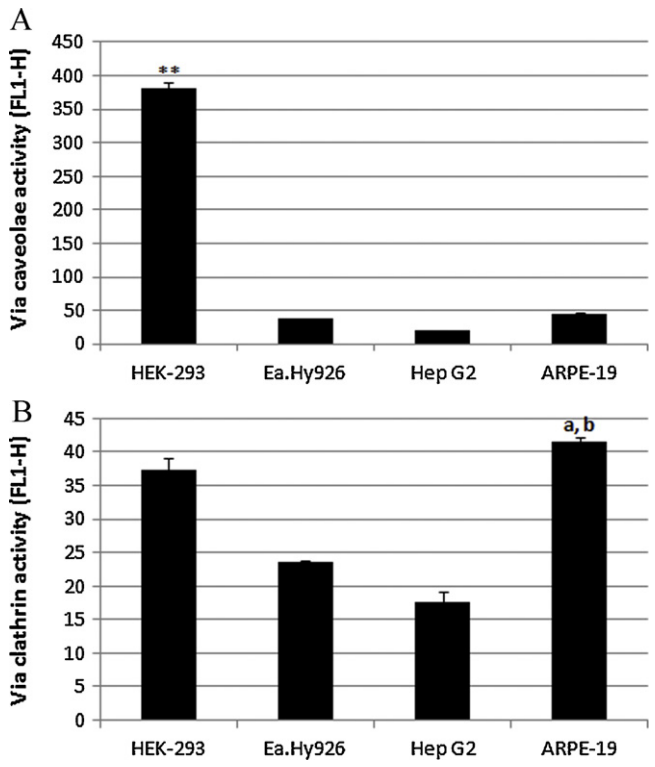

Fig. 3. Caveolae (A) and clathrin (B) mediated endocytosis activity in different cell lines. AlexaFluor488-Cholera Toxin and AlexaFluor488-Transferrin was quantified by flow cytometry by measuring the fluorescence of AlexaFluor488 at 525 nm (FL1-H). The SLN to DNA ratio (w/w) was 5:1 and the dextran–protamine to DNA ratio 1:2:1. Error bars represent S.D. ($n = 9$). $^{**}p < 0.01$ with respect to other cell lines. $^{a}p < 0.01$ with respect to Ea.Hy926 and HepG2. $^{b}p < 0.05$ respect to HEK-293 cells.

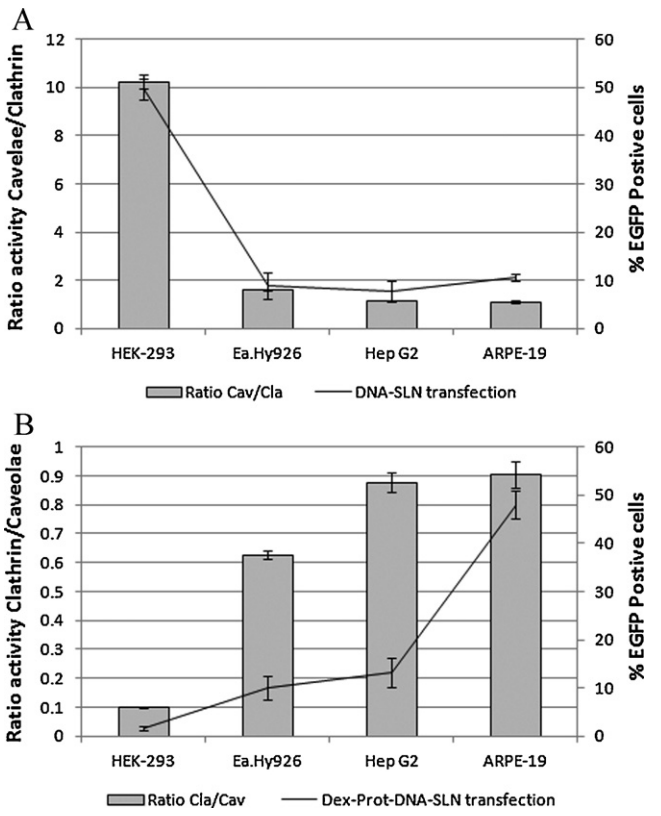

Fig. 4. Relation between transfection of the DNA–SLN vector and ratio caveolae/clathrin endocytosis activity (A); relation between transfection of the Dex–Prot–DNA–SLN vector and the ratio clathrin/caveolae endocytosis activity (B). The SLN to DNA ratio (w/w) was 5:1 and the dextran–protamine to DNA ratio 1:2:1. Error bars represent S.D. ($n = 9$).

cells was much lower. When cells were treated with the clathrin-mediated endocytosis marker, ARPE-19 cells showed the highest activity, although differences among the cell lines were lower than the caveolae endocytosis activity (Fig. 3B).

A balance between endocytosis *via* caveolae and *via* clathrin (ratio activity aprox. = 1) was observed in all cell lines except in HEK-293, which showed higher caveolae-mediated endocytosis (Fig. 4A and B).

3.5. Interaction with erythrocytes

Agglutination was evaluated by incubating erythrocytes with the vectors. Fig. 5C shows a light agglutination when erythrocytes were in touch with the DNA–SLN vector. The use of the Dex–Prot–DNA–SLN vector caused no agglutination, though (Fig. 5E). The same study was carried out with the Prot:DNA:SLN vector (w/w/w 2:1:5 ratio) and a light agglutination was detected (Fig. 5D). Fig. 6 features the hemolysis activity of erythrocytes after treatment with the vectors. As can be seen, neither of the vectors induced hemolysis.

3.6. In vivo transfection

Free DNA and the Dex–Prot–DNA–SLN vector were intravenously administered to mice. In order to ensure that the observed green fluorescence was not an artifact of the immunolabeling, we subjected samples of mice treated with the vector without the plasmid (empty vector) to the same procedure with the primary and the secondary antibodies. No green fluorescence and no evidence of toxicity were detected.

Mice were sacrificed 3 or 7 days after the intravenous administration. Twelve sections from each tissue, representing the whole organ, were analyzed (Fig. 7). EGFP fluorescence in the tissue sections of mice treated with free DNA was not observed. However, EGFP was detected in the liver, spleen and lung of the mice treated with the Dex–Prot–DNA–SLN vector. At day 3, almost all sections of liver, spleen and lungs showed EGFP. Transfection still remained high in hepatic, splenic and lung sections 7 days after intravenous administration. Fig. 8 shows images of the tissues where EGFP was present.

4. Discussion

The successful development of effective non-viral delivery systems is one of the most important goals in the field of gene therapy. Gene delivery efficacy depends on their ability to form stable complexes with nucleic acids, to feature low cytotoxicity, and to disassemble intracellularly in order to release the nucleic acid (Gascón and Pedraz, 2008). In previous work, we developed solid lipid nanoparticles (SLN) as a non-viral vector that was able to induce the expression of the green fluorescent protein after the intravenous administration to mice (del Pozo-Rodríguez et al., 2010). In the present study we have evaluated the transfection capacity of a new vector consisting of SLN, protamine and dextran after systemic administration to mice. In order to better assess the role of dextran and protamine in the transfection process, we also compared the behavior of the Dex–Prot–DNA–SLN vector and the DNA–SLN vector in four cell lines *in vitro*.

Precondensing the plasmid with protamine contributes to protecting it against DNase degradation since this small peptide (Mw 4000–4250) is an efficient DNA condenser. Moreover, protamine presents nuclear localization signals (NLS) with high arginine content that enhances the entry of DNA into the nucleus (Sorgi et al.,

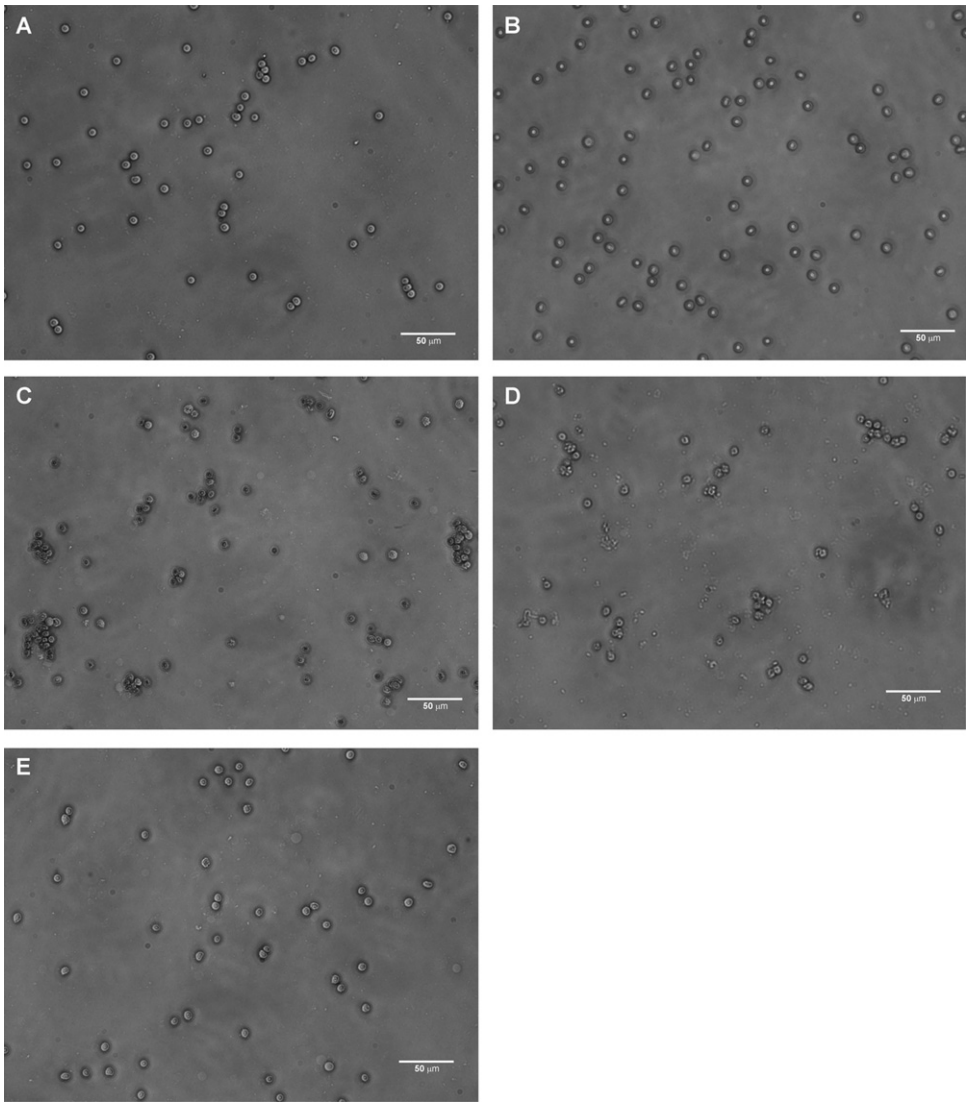

Fig. 5. Agglutination of erythrocytes when blood is untreated (A), treated with DNA (B), DNA–SLN vector (C), protamine–DNA–SLN vector (D) and dextran–protamine–DNA–SLN vector (E).

1997; Ye et al., 2008). This arginine content has previously shown an enhancement of viral and non-viral gene delivery systems (Lanuti et al., 1999), although it has not responded positively when used alone (Xu et al., 2008). Dextran is a polyanion biocompatible polysaccharide that hampers interactions with other components such as serum proteins (Maruyama et al., 2004) and could be beneficial for transfection, especially *in vivo* (Finsinger et al., 2000).

Vectors were characterized in terms of size and superficial charge. The addition of protamine and dextran to the SLN did not modify either the size or the surface charge (Table 1). Particle size depends on the balance between the ability of the peptide to precondense DNA, which would imply a reduction in size, and the space the peptide itself occupies. Thus, a change in the particle size does not always happen (del Pozo-Rodríguez et al., 2009). Regarding superficial charge, since protamine is positively charged and dextran has negative charges, the addition of these components does not imply a change in the surface charge of the complexes.

Although there was no difference in particle size and surface charge, vectors showed differences in transfection capacity *in vitro*. Transfection studies were carried out in established

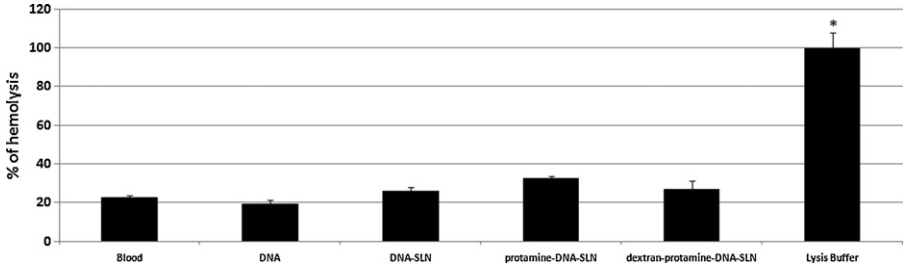

Fig. 6. Hemolysis activity of erythrocytes after treatment with the vectors. Lysis buffer represents 100% hemolysis sample. Error bars represent S.D. ($n = 9$). $^{*}p < 0.01$.

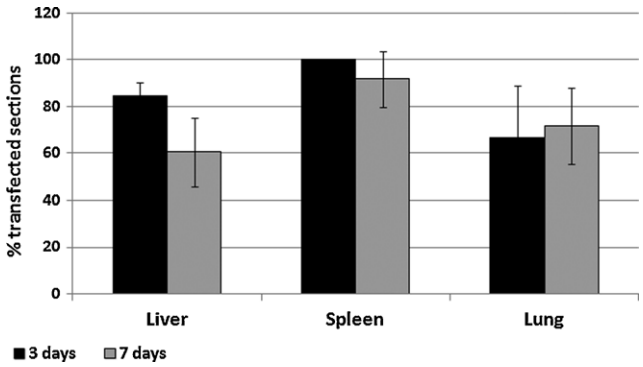

Fig. 7. *In vivo* transfection expressed as percentage of transfected sections in liver, spleen and lung treated with DNA–SLN, and Dex–Prot–DNA–SLN vectors. The SLN to DNA ratio (w/w) was 5:1 and the dextran–protamine to DNA ratio 1:2:1. A = on day 3 post-transfection. B = on day 7 post-transfection. Error bars represent S.D. ($n = 3$).

cells from different human origin: kidney (HEK-293), vascular endothelium (Ea.hy926), liver (Hep G2) or retina (ARPE-19). The Dex–Prot–DNA–SLN vector induced hardly any transfection in HEK-293 cells, but it had a very good response in ARPE-19 cells (almost 50% of positive cells). On the contrary, the DNA–SLN vector transfected HEK-293 cells efficiently (up to 52% of EGFP positive cells), whereas in retinal cells, the transfection level was significantly lower (10%). Both the Dex–Prot–DNA–SLN and the DNA–SLN vectors induced modest transfection in Ea.hy926 and Hep G2 cell lines (about 10% transfected cells).

It is known that transfection is conditioned by the entry and intracellular trafficking of the vectors, which are cell line dependent processes (Li et al., 2004; von Gersdorff et al., 2006). In order to better understand the differences in cell transfection of the two formulations, we studied the cell uptake of the vectors in the four cell lines by means of flow cytometry. No differences in cell uptake that could justify the differences in cell transfection were found (Fig. 2). We also studied which endocytosis mechanisms (clathrin- or caveolae-mediated endocytosis) were available in the four cell lines. Fig. 3A depicts that in the HEK-293 cell, the *via* caveolae/rafts presents a higher activity than in the other cell lines ($p < 0.01$). However, the differences in the activity of clathrin-mediated endocytosis between the four cell lines were less pronounced (Fig. 3B). When we related transfection and endocytosis activity, we observed that the DNA–SLN vector only transfected efficiently HEK-293 (>50% positive cells), cells in which caveolae activity was much higher than clathrin activity (ratio of caveolae/clathrin activity >10). This seems to indicate a relationship between transfection capacity of this vector and the caveolae activity.

In contrast, the Dex–Prot–DNA–SLN vector hardly transfected HEK-293 cells but its transfection was higher in the other cell lines, in which the clathrin/caveolae activity ratio was also higher. These results are consistent with a previous study (Delgado et al., 2011), in which we showed that the lysosomal activity seemed to be necessary to release the complex protamine–DNA from the SLN and, consequently, to transfect the cells. This lysosomal activity is avoided when endocytosis *via* caveolae is used by the vectors but not when they enter the cells *via* clathrin. Therefore, the low activity of clathrin-mediated endocytosis in HEK-293 in comparison with caveolae-mediated endocytosis may justify the low transfection level achieved with the Dex–Prot–DNA–SLN vector in this cell line. Differences in transfection levels between Ea.Hy926, Hep G2 and ARPE-19 cells, are not only related to clathrin and caveolae activity; it is well known that besides entry, other cell line-dependent factors (diffusion in the cytoplasm, cell division rate, entrance in the nucleus, *etc.*) are involved in transfection process.

After intravenous administration to mice, lipid nanoparticles with protamine and dextran reached a significant response in liver, spleen and lungs. Three days after the administration of the formulation the percentage of positive sections (presence of EGFP) was 70% in lungs, 85% in liver and 100% in spleen. Transfection was still detected in the three organs 7 days post-administration, and it even increased in lungs. The formulation DNA–SLN, previously assayed in mice by intravenous route (del Pozo-Rodríguez et al., 2010), also showed transfection in liver and spleen but not in lungs. Moreover, protein expression highly decreased 7 days after administration. These results suggest a longer circulation time of the Dex–Prot–DNA–SLN vector in comparison with the DNA–SLN vector (Chrastina et al., 2011; Fischer et al., 2004). It is well known that positive charges of cationic complexes may interact with other lipid particles, serum proteins and erythrocytes, leading to aggregation in the blood stream and hemagglutination (Eliyahu et al., 2002) and, consequently, to high clearance from the circulation. This is why, prior the *in vivo* evaluation, we studied the erythrocytes agglutination capacity and the potential hemolytic activity of the vectors. The DNA–SLN vector showed low hemagglutination capacity, whereas Dex–Prot–DNA–SLN showed no agglutination (Fig. 5). We also detected hemagglutination with a formulation consisting of protamine, DNA and SLN at the 2:1:5 ratio. This indicates that the lack of hemagglutination effect of the Dex–Prot–DNA–SLN probably is due to the presence of dextran on the nanoparticle surface. Hemolytic activity, which is also indicative of cytotoxicity, was negligible with all the formulations. Therefore, the longer circulation stay of the Dex–Prot–DNA–SLN vector in the bloodstream may be partially related to the presence of dextran on the nanoparticle surface. The surface features of this new vector may also induce a lower opsonization and a slower uptake by the RES. Moreover, the high DNA condensation of protamine that contributes to the nuclease resistance may result in an extended stay of plasmid in the organism. The presence of NLS in protamine, which improves the nuclear envelope translocation, and its capacity to facilitate transcription (Masuda et al., 2005) may also improve the transfection efficacy *in vivo*.

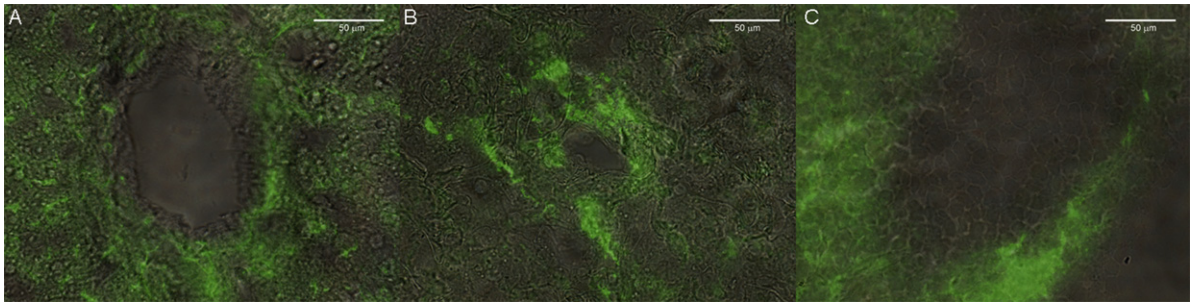

Fig. 8. Fluorescence microscopy images of transfected sections of liver (A), lung (B) and spleen (C) after the immunolabelling of EGFP (green). Images were captured at 40×.

The anatomical and physiological characteristics of liver and spleen, more specifically the discontinuous endothelium, facilitate the uptake of the nanoparticles and contribute to efficiently transfect these organs. These results suggest the potential usefulness of this vector when liver and spleen are the target organs (Chrastina et al., 2011), for example, in the treatment of diseases such as liver or spleen tumors (Tang et al., 2008), hepatitis B (Zhang et al., 2007) or for the design of DNA vaccines (Raska et al., 2008). The liver could also be used as a depot organ to produce large amounts of a therapeutic enzyme that is secreted to the bloodstream and recaptured by other organs (Mango et al., 2004). The ability of our new vector to transfect in lungs makes it useful as a potential system for the treatment of diseases such as acute respiratory distress syndrome (ARDS), cancer, asthma, emphysema and cystic fibrosis (CF) (Griesenbach and Alton, 2009).

5. Conclusions

We have developed a new vector that induced the expression of the EGFP *in vivo* during at least 7 days after intravenous administration to mice. Although in recent years the development of carriers to target caveolae-mediated endocytosis is emerging as an strategy to improve non-viral vectors (Chrastina et al., 2011; Liu et al., 2011; Sahay et al., 2010), our vector provides high transfection levels in culture cells when it is internalized *via* clathrin. In spite of the promising results, additional studies are needed to assess the real potential of this new vector. The lack of adequate methods to better understand the process of endocytosis and intracellular trafficking of gene delivery systems *in vivo* (Sahay et al., 2010) justifies the need to evaluate these products in animal models during early stages of the development process.

Acknowledgement

This work was supported by the Basque Government's Department of Education, Universities and Investigation (IT-341-10).

References

Borgia, S.L., Regehly, M., Sivaramakrishan, R., Mehnert, W., Korting, H.C., Danker, K., et al., 2005. Lipid nanoparticles for skin penetration enhancement—correlation to drug localization within the particle matrix as determined by fluorescence and parelectric spectroscopy. J. Control. Release 110, 151–163.

Chrastina, A., Kerri, A.M., Schnitzer, J.E., 2011. Overcoming *in vivo* barriers to targeted nanodelivery. Wiley Interdiscip. Rev. Nanomed. Nanobiotechnol. 3, 421–437.

del Pozo-Rodríguez, A., Delgado, D., Solinís, M.A., Gascón, A.R., Pedraz, J.L., 2007. Solid lipid nanoparticles: formulation factors affecting cell transfection capacity. Int. J. Pharm. 339, 261–268.

del Pozo-Rodríguez, A., Delgado, D., Solinís, M.A., Gascón, A.R., Pedraz, J.L., 2008. Solid lipid nanoparticles for retinal gene therapy: transfection and intracellular trafficking in RPE cells. Int. J. Pharm. 360, 177–183.

del Pozo-Rodríguez, A., Pujals, S., Delgado, D., Solinís, M.A., Gascón, A.R., Giralt, E., et al., 2009. A proline-rich peptide improves cell transfection of solid lipid nanoparticle-based non-viral vectors. J. Control. Release 133, 52–59.

del Pozo-Rodríguez, A., Delgado, D., Solinís, M.A., Pedraz, J.L., Echevarria, E., Rodríguez, J.M., et al., 2010. Solid lipid nanoparticles as potential tools for gene therapy: *in vivo* protein expression after intravenous administration. Int. J. Pharm. 385, 157–162.

del Pozo-Rodríguez, A., Delgado, D., Solinís, M.A., Gascón, A.R., 2011. Lipid nanoparticles as vehicles for macromolecules: nucleic acids and peptides. Recent Pat. Drug. Deliv. Formul. 5, 214–226.

Delgado, D., del Pozo-Rodríguez, A., Solinís, M.A., Gascón, A.R., 2011. Understanding the mechanism of protamine in solid lipid nanoparticle-based lipofection: the importance of the entry pathway. Eur. J. Pharm. Biopharm. 79, 495–502.

Delgado, D., del Pozo-Rodríguez, A., Solinís, M.A., Avilés, M., Weber, B.H.F., Fernández, E., Gascón A.R., 2012. Dextran and protamine-based solid lipid nanoparticles as potential vectors for the treatment of X linked juvenile retinoschisis, submitted for publication.

Eliyahu, H., Servel, N., Domb, A.J., Barenholz, Y., 2002. Lipoplex-induced hemmagglutiantion: potential involvement in intravenous gene delivery. Gene Ther. 9, 850–858.

Finsinger, D., Remy, J.S., Erbacher, P., Koch, C., Plank, C., 2000. Protective copolymers for nonviral gene vectors: synthesis, vector characterization and application in gene delivery. Gene Ther. 7, 1183–1192.

Fischer, D., Osburg, B., Pertersen, H., Kissel, T., Bickel, U., 2004. Effect of poly(ethylene imine) molecular weight and pegylation on organ distribution and pharmacokinetics of polyplexes with oligodeoxynucleotides in mice. Drug Metab. Dispos. 32, 983–992.

Gascón, A.R., Pedraz, J.L., 2008. Cationic lipids as gene transfer agents: a patent review. Expert Opin. Ther. Pat. 18, 515–524.

Gascón, A.R., Solinís, M.A., del Pozo-Rodríguez, A., Delgado, D., Pedraz, J.L., 2011. Lipid nanoparticles for gene therapy. WO2011015701.

Griesenbach, U., Alton, E.W., 2009. Cystic fibrosis gene therapy: successes, failures and hopes for the future. Expert Rev. Respir. Med. 3, 363–371.

Gupta, B., Levchenko, T.S., Torchilin, V.P., 2005. Intracellular delivery of large molecules and small particles by cell-penetrating proteins and peptides. Adv. Drug Deliv. Rev. 57, 637–651.

Gupta, B., Levchenko, T.S., Torchilin, V.P., 2007. TAT peptide-modified liposomes provide enhanced gene delivery to intracranial human brain tumor xenografts in nude mice. Oncol. Res. 16, 351–359.

Hoare, M., Greiser, U., Schu, S., Mashayekhi, K., Aydogan, E., Murphy, M., et al., 2010. Enhanced lipoplex-mediated gene expression in mesenchymal stem cells using reiterated nuclear localization sequence peptides. J. Gene Med. 12, 207–218.

Koyanova, R., Tenchov, B., 2011. Recent patents in cationic lipid carriers for delivery of nucleic acids. Recent Pat. DNA Gene. Seq. 5, 8–27.

Kurosaki, T., Kitahara, T., Fumoto, S., Nishida, K., Yamamoto, K., Nakagawa, H., et al., 2010. Chondroitin sulfate capsule system for efficient and secure gene delivery. J. Pharm. Pharm. Sci. 13, 351–361.

Lanuti, M., Kouri, C.E., Force, S., Chang, M., Amin, K., Xu, K., et al., 1999. Use of protamine to augment adenovirus-mediated cancer gene therapy. Gene Ther. 6, 1600–1610.

Li, W.H., Ishida, T., Tachibana, R., Almofti, M.R., Wang, X.Y., Kiwada, H., 2004. Cell type-specific gene expression, mediated by TFL-3, a cationic liposomal vector, is controlled by a post-transcription process of delivered plasmid DNA. Int. J. Pharm. 276, 67–74.

Liu, C., Yu, W., Chen, Z., Zhang, J., Zhang, J.N., 2011. Enhanced gene transfection efficiency in CD13-positive vascular endothelial cells with targeted poly(lactic acid)–poly(ethylene glycol) nanoparticles through caveolae-mediated endocytosis. J. Control. Release 151, 162–175.

Liu, F., Shollenberg, L.M., Conwell, C.C., Yuan, X., Huang, L., 2007. Mechanism of naked DNA clearance after intravenous injection. J. Gene Med. 9, 613–619.

Ma, B., Zhang, S., Jiang, H., Zhao, B., Lv, H., 2007. Lipoplex morphologies and their influences on transfection efficiency in gene delivery. J. Control. Release 123, 184–194.

Mango, R.L., Xu, L., Sands, M.S., Vogler, C., Seiler, G., Schwarz, T., et al., 2004. Neonatal retroviral vector-mediated hepatic gene therapy reduces bone, joint, and cartilage disease in mucopolysaccharidosis VII mice and dogs. Mol. Genet. Metab. 82, 4–19.

Maruyama, K., Iwasaki, F., Takizawa, T., Yanagie, H., Niidome, T., Yamada, E., et al., 2004. Novel receptor-mediated gene delivery system comprising plasmid/protamine/sugar-containing polyanion ternary complex. Biomaterials 25, 3267–3273.

Masuda, T., Akita, H., Harashima, H., 2005. Evaluation of nuclear transfer and transcription of plasmid DNA condensed with protamine by microinjection: the use of a nuclear transfer score. FEBS Lett. 579, 2143–2148.

Morille, M., Passirani, C., Vonarbourg, A., Clavreul, A., Benoit, J.P., 2008. Progress in developing cationic vectors for non-viral systemic gene therapy against cancer. Biomaterials 29, 3477–3496.

Noone, P.G., Hohneker, K.W., Zhou, Z., Johnson, L.G., Foy, C., Gipson, C., et al., 2000. Safety and biological efficacy of a lipid–CFTR complex for gene transfer in the nasal epithelium of adult patients with cystic fibrosis. Mol. Ther. 1, 105–114.

Porteous, D.J., Dorin, J.R., McLachlan, G., Davidson-Smith, H., Davidson, H., Stevenson, B.J., et al., 1997. Evidence for safety and efficacy of DOTAP cationic liposome mediated CFTR gene transfer to the nasal epithelium of patients with cystic fibrosis. Gene Ther. 4, 210–218.

Raska, M., Moldoveanu, Z., Novak, J., Hel, Z., Novak, L., Bozja, J., et al., 2008. Delivery of DNA HIV-1 vaccine to the liver induces high and long-lasting humoral immune responses. Vaccine 26, 1541–1551.

Rejman, J., Bragonzi, A., Conese, M., 2005. Role of clathrin- and caveolae mediated endocytosis in gene transfer mediated by lipo- and polyplexes. Mol. Ther. 12, 468–474.

Sahay, G., Alakhova, D.Y., Kavanov, A.V., 2010. Endocytosis of nanomedicines. J. Control. Release 145, 182–195.

Sorgi, F.L., Bhattacharya, S., Huang, L., 1997. Protamine sulfate enhances lipid-mediated gene transfer. Gene Ther. 4, 961–968.

Tang, H., Tang, X.Y., Liu, M., Li, X., 2008. Targeting alpha-fetoprotein represses the proliferation of hepatoma cells via regulation of the cell cycle. Clin. Chim. Acta 394, 81–88.

Varkouhi, A.K., Scholte, M., Storm, G., Haisma, H.J., 2010. Endosomal escape pathways for delivery of biological. J. Control. Release 151, 220–228.

von Gersdorff, K., Sanders, N.N., Vandenbroucke, R., De Smedt, S.C., Wagner, E., Ogris, M., 2006. The internalization route resulting in successful gene expression depends on polyethylenimine both cell line and polyplex type. Mol. Ther. 14, 745–753.

Xu, Z., Gu, W., Chen, L., Gao, Y., Zhang, Z., Li, Y., 2008. A smart nanoassembly consisting of acid-labile vinyl ether PEG-DOPE and protamine for gene delivery: preparation and *in vitro* transfection. Biomacromolecules 9, 3119–3126.

Ye, J., Wang, A., Liu, C., Chen, Z., Zhang, N., 2008. Anionic solid lipid nanoparticles supported on protamine/DNA complexes. Nanotechnology 19, 285708.
Yoshida, J., Mizuno, M., Fuji, M., Kajita, Y., Nakahara, N., Hatano, M., et al., 2004. Human gene therapy for malignant gliomas (glioblastoma multiforme and anaplastic astrocytoma) by *in vivo* transduction with human interferon beta gene using cationic liposomes. Hum. Gene Ther. 15, 77–86.
Zanta, M.A., Belguise-Valladier, P., Behr, J.P., 1999. Gene delivery: a single nuclear localization signal peptide is sufficient to carry DNA to the cell nucleus. Proc. Natl. Acad. Sci. U.S.A. 96, 91–96.
Zhang, Y., Rong Qi, X., Gao, Y., Wei, L., Maitani, Y., Nagai, T., 2007. Mechanisms of co-modified liver-targeting liposomes as gene delivery carriers based on cellular uptake and antigens inhibition effect. J. Control. Release 117, 281–290.